Corresponding Author:

Christopher Gold

Department of Land Surveying and Geo-Informatics
Hong Kong Polytechnic University
Hung Hom, Kowloon, Hong Kong

Key words:

Terrain modelling; Delaunay/Voronoi diagrams; Contour lines; skeleton; generalization.

Terrain Reconstruction from Contours by Skeleton Construction

D. Thibault [1] and C. M. Gold [1, 2]

[1] Centre for Research in Geomatics
Laval University, Quebec City, Qc, Canada
E-mail: d.thibault@tecsult.com, ChristopherGold@Voronoi.com

[2] Department of Land Surveying and Geo-Informatics
Hong Kong Polytechnic University, Hung Hom, Kowloon, Hong Kong

ABSTRACT: Generating terrain models from contour input is still an important process. Most methods have been unsatisfactory, as they either do not preserve the form of minor ridges and valleys, or else they are poor at modelling slopes. A method is described here, based on curve extraction and generalization techniques, that is guaranteed to preserve the topological relationships between curve segments. The skeleton, or Medial Axis Transform, can be extracted from the Voronoi diagram of a well-sampled contour map and used to extract additional points that eliminate cases of "flat triangles" in a triangulation. Elevation estimates may be made at these points. Based on this approach it is possible to make reasonable estimates of slopes for terrain models, and to extract meaningful intermediate points for triangulated irregular networks (TINs).

1. INTRODUCTION

Despite the development of modern satellite systems, a great deal of the world's database of terrain elevation is in the form of contour overlays from traditional mapping agencies. These have the advantage that they were developed using human understanding of the observed landforms, but the disadvantage that they are not easily converted to a useful digital format. Due to the high cost of direct methods for terrain capture, cartographic documents such as contours maps and profiles are often preferred [19].

The usual methods for generating a terrain model from contour lines consist either of interpolation onto a grid, or of the construction of a triangulation of points on the contour lines. Carrara et al. [5] discuss different techniques for generating digital terrain models from contour lines. The errors in gridded data are well known, in particular the difficulty of producing a suitable set of neighbouring data points for the weighted-average function often used. This is particularly pronounced when the data is ill-distributed, as is the case with ships' paths, aircraft flight lines, digitized contours, etc. The use of Voronoi diagrams and "area-stealing" or natural-neighbour interpolation has been shown to adapt well to poor data distributions [7] because the insertion into the mesh of a sampling point generates a well- defined set of neighbours, which may be few or many, and the areas stolen from these neighbouring Voronoi cells act as a well-behaved weighting function. Triangulation methods, the main topic of this article, depend both on the selection of correct triangle edges between points on the contours, and the generation of sufficient additional points to correctly form ridges, valleys, peaks and pits. Garcia et al.[6] discuss the triangulation of contour input.

2. PREVIOUS WORK

Triangulation methods (TINs) have been popular for some years, and have the advantage of being adaptive to the data distribution. They are usually based on the Delaunay triangulation, the dual of the Voronoi tessellation. These can be extremely effective, but are not always ideal for contour input. They may give a very angular surface, and it is not easy to ensure that they connect adjacent contour lines correctly. If the contours are too close, or the sampling along the contour is inadequate, triangle edges may cross contour lines. If there are re-entrants or promontories in a contour line, then the three triangle vertices may have the same elevation, and are unable to mimic the human perception of a minor ridge or valley as a cause. Robinson [18] presents a method to fix this problem by changing the diagonal of triangle pairs. Similar problems arise at peaks and pits.

Another issue of note is the estimation (and perception) of slope based on the contour lines. Any method of interpolation that makes a poor choice of neighbours for a weighted average will first of all have a deleterious effect on the perceived slope of the resulting model**.** [18] also discusses various techniques that partially take account of slope information at contours. TINs often have widely variable slope between adjacent triangles, yet it is obvious that the line of maximum slope is perpendicular to each contour line segment. Interpolation techniques, in particular, often generate a zero slope at each data point - giving a terraced or staircase effect to a terrain model derived from contours. Thus current methods are theoretically unsatisfactory although it may be possible to assign slopes to data points prior to interpolation [7].

This paper will attempt to examine both the problem of generating intermediate points for valid triangulations of contours in the regions of ridges, summits, etc., as well as addressing the question of the valid estimation of slopes at contour lines. This depends on an understanding of the primal/dual relationships of the generating Delaunay/Voronoi structures, and recent methods for extracting curves from unordered input data, such as scanned maps

3. CURVE EXTRACTION

Given that the Voronoi/Delaunay construction satisfactorily adapts to varying data distributions, this was taken as our baseline model for preserving topological relationships. Okabe et al. [17] provide an excellent summary of Voronoi diagrams and applications. Figure 1 shows a simple Voronoi diagram, together with adjacency relationships.

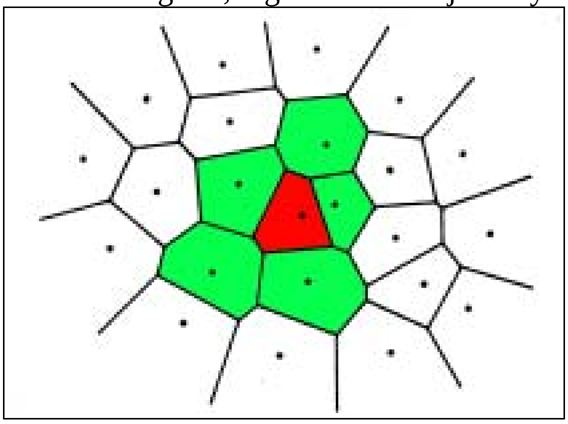

Figure 1 A simple Voronoi diagram. The green cells are the Voronoi neighbours of the red cell.

The work described here is a continuation of our previous efforts [11] [8] [9] on data input. Briefly, in the first paper we developed a digitizing technique for forest polygons based on digitizing around the interiors of each polygon, giving the points the labels of the polygons they fall in, creating the Voronoi diagram, and extracting the Voronoi boundaries between points with different labels. This was rapid, and guaranteed to be topologically correct. In the second paper we extended this to scanned maps, by deriving “fringe” points on the interior of each polygon by image filtering, labelling these points with a floodfill algorithm, and extracting the polygon boundaries as just mentioned. In the third paper we show that the work of Guibas and Stolfi [14] in developing the Quad-Edge structure, may be extended to connected maps by permitting the simple edge between two vertices to become an arc (the “Quad-Arc”), with multiple points along it.

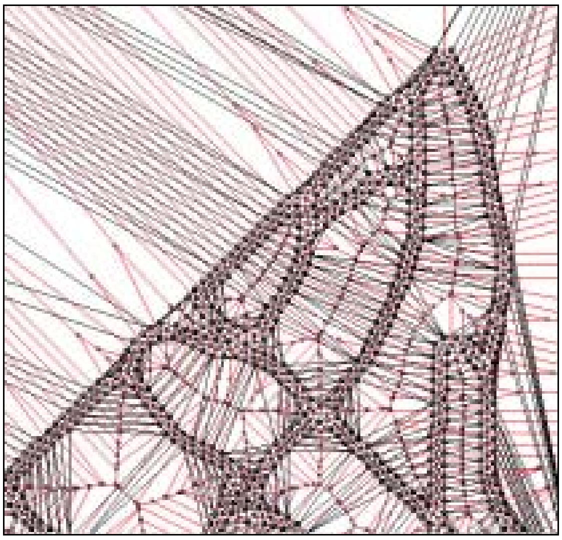

Figure 2 A portion of a scanned forest map.

The properties of the Quad-Edge/Quad-Arc led us to look at our previous techniques. The Quad-Arc allows the management of any connected graph on the plane or orientable manifold. However, our earlier algorithms required closed polygons, with different labels, in order to identify the edges we wished to preserve. Thus unclosed linework would be lost, as the polygon label would be the same on both sides of the line. However, we could not find a satisfactory algorithm based on point distribution alone, without some labelling function.

Our first problem was then to re-examine the problem of ensuring that all contour line segments were part of the Delaunay triangulation – or, at least, to know the required sampling density in order to guarantee that property. This could be considered as a special case of curve extraction from unordered input data.

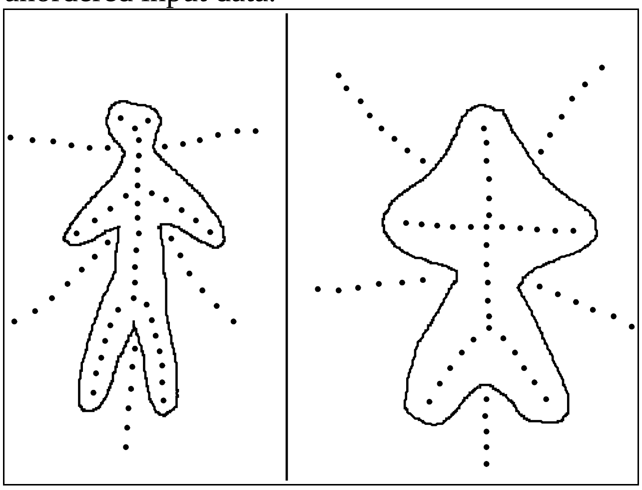

Figure 3 Endo- and exo-skeletons. (After Blum, 1967)

Gold et al. [11] worked on this for polygon maps, and Gold [8] for scanned maps, where "fringe" points were generated on each side of the boundary, the Delaunay triangulation constructed, and the "skeleton" of Voronoi edges between the two rows of fringe points was extracted (Figure 2). Blum [4] defined the skeleton, or Medial Axis Transform (MAT), for irregular "biological" shapes (see Figure 3), based on the "wave-front" or "prairie fire" analogy, with the MAT formed where wave-fronts meet. Each point on the MAT of a continuous shape is the centre of a disc touching the boundary at at least two locations – thus the shape may be reconstructed from the union of al the MAT discs. (It should be noted that in the case of the discretely-sampled skeleton the discs must touch at least three sample points.)

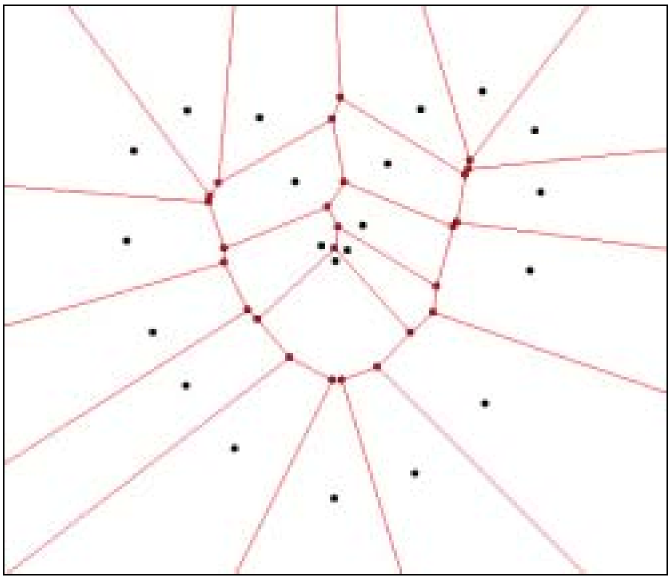

Figure 4 The Voronoi diagram of a boundary point set

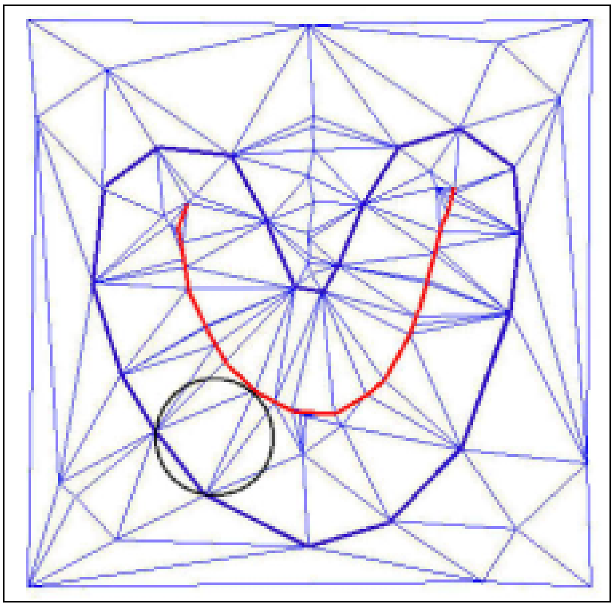

Figure 5 Amenta et al.'s construction for crust extraction

In 1998 Amenta et al. published a seminal article [2] where they showed that the connected set of boundary points (the "crust") could be extracted using the Voronoi diagram. Their insight was that eliminating all Delaunay edges that crossed the skeleton of the polygonal object under consideration would leave the remaining edges to form the crust. Figure 4 shows the Voronoi diagram of a set of boundary points. As each edge of the Delaunay triangulation is associated with a perpendicular edge in the Voronoi diagram, eliminating all the Delaunay edges that cross the skeleton of the shape leaves the Delaunay edges that form the shape boundary. They achieved this by first generating the Voronoi diagram of the boundary points, and exporting the Voronoi vertices. In a second step, they constructed the Delaunay triangulation of both the original boundary points and the new Voronoi vertices (Figure 5). Any Delaunay edge connecting two boundary points must be part of the desired crust, as Delaunay edges that originally crossed from one side of the polygon to the other would now be cut by the newly-inserted "skeleton" points formed from the original Voronoi vertices. They showed that if the samples along the boundary were not more than (approximately) 0.25 times the distance to the skeleton, it was guaranteed that the complete crust (and no other edges) would be preserved.

However, our previous work had used the skeleton (a subset of the Voronoi edges) to define our topologically complete polygon boundaries, as in Figure 2, not the crust. Gold [10] and Gold and Snoeyink [12] showed that the two steps were unnecessary - a local test of associated Voronoi/Delaunay edge pairs sufficed. The work of Amenta et al. reduced to a simple test on each Delaunay edge of the original Voronoi/Delaunay diagram. Thus it was possible to generate both the crust and the skeleton in one step, as a simple test on each Voronoi/Delaunay edge pair. Essentially, each edge pair (stored as the Quad-Edge structure of [14]) would be assigned either to the crust or the skeleton.

In order to use our skeleton-based generalization algorithm, we needed a structure that was capable of managing both the primal and the dual graph with equal felicity, and that could apply to simple Delaunay/Voronoi structures as well as to polygon arcs. Since we were often working interchangeably with Delaunay/Voronoi representations, the Quad-Edge data structure of [14] became an obvious candidate. It has various attractions: it is a method for representing the edge connectedness of any connected graph on a manifold; it is symmetric in its storage of both the primal and the dual edge; it has a complete algebra associated with it, requiring no searches around polygons, nodes, etc.; and it is admirably adapted to an object-oriented programming environment. There are only two operations: Make-Edge to create a new edge, and Splice to connect or disconnect two ends. Gold [9] shows a half-page of code that implements the basic operations. To us it appears the most elegant structure. One limitation is that it works only for connected graphs. If there are "islands" in a polygon map, for example, and the arcs between the nodes in the data structure graph correspond to the polygon edges in the map, then the presence of the island within some other polygon can not be detected without further processing. The Voronoi diagram, being space-covering, does not have this problem, and islands may be connected to their enclosing polygon during extraction from the original Voronoi diagram.

In [10] a simplified method of the technique of Amenta et al. was described, which depended only on the local testing of associated Voronoi/Delaunay edge pairs. As seen in Figure 4, the result of the Amenta construction was to guarantee that each crust edge had a circumcircle that was not only empty of other “black” data points (the usual Delaunay condition), but also of red Voronoi vertices as well. This reduced the problem to a local test of Voronoi/Delaunay edge pairs: each pair would be drawn as a Delaunay edge (crust), or as a Voronoi edge (skeleton), but not both. The test simply stated that, for a Delaunay edge to be considered part of the crust, a circle must exist through its two vertices that does not contain any Voronoi vertices, as drawn in Figure 5. Otherwise the associated Voronoi edge is part of the skeleton. Figure 6 illustrates the rule.

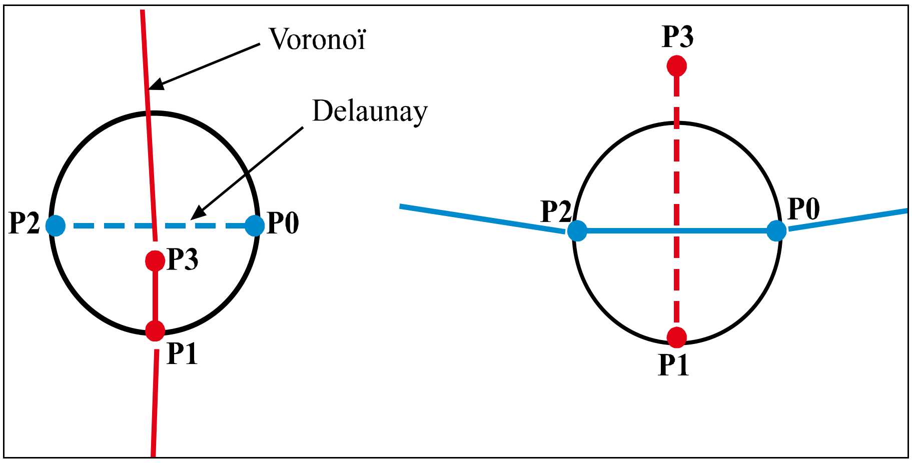

Figure 6 The Delaunay edge P0-P2 has no circle empty of Voronoi vertices in the example on the left - hence its dual P1-P3 is part of the skeleton. On the right the empty circle indicates that the Delaunay edge is part of the crust.

This directly resolved our interest in skeleton generation, but, of even more importance, both the crust and the skeleton could be generated at the same time, and the relationships between them preserved. Figure 7 shows the crust and skeleton for the simple polygon of Figure 4. Each of the crust (boundary) edges drawn is a Delaunay edge, because of the previously-mentioned empty circle condition, and the associated Voronoi edge (passing between the two Delaunay vertices) is suppressed. Similarly, the skeleton (or medial axis) consists of those Delaunay edges that failed the circle test, and in this case the dual Voronoi edge is drawn, and the Delaunay edge suppressed.

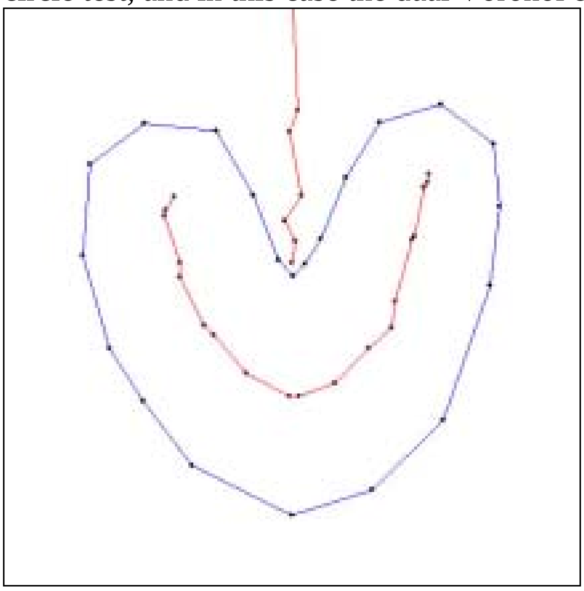

Figure 7 Simultaneous extraction of the crust and skeleton for the data of Figure 4

Figure 8 shows the result for the scanned image of a maple leaf. The resulting form is, in general, quite satisfactory, except at some sharp corners, where the sampling is not sufficient. Amenta et al. defined an "r-sampled" curve as one where, for any point on the curve, there is a sample point within r times the distance from that point to the skeleton. They showed that, in order to guarantee both that all crust points were connected, and that no non-crust points were connected, the value of r had to be less than 0.252. Some of the corners of the maple leaf are very sharp, meaning that the skeleton approaches the crust very closely, requiring a very high sample density to resolve the connections correctly. Gold and Snoeyink [12] as well as giving a local proof of the theorems, showed that the value of r may be as high as 0.42 – although this is not yet optimal.

An additional difference between the work of Amenta et al. and this work is that in our work the boundary was generated from an image, and therefore has a certain positional sampling error. This is reflected in the “hairs” on the skeleton, which are formed whenever three adjacent vertices on the crust form a Delaunay triangle having an empty circumcircle. This is equivalent to one form of “flat triangle” found in the processing of contour maps. It would be desirable to trim these skeleton hairs. Gold [10] shows that this can be achieved by “retracting” the leaves of this skeleton.

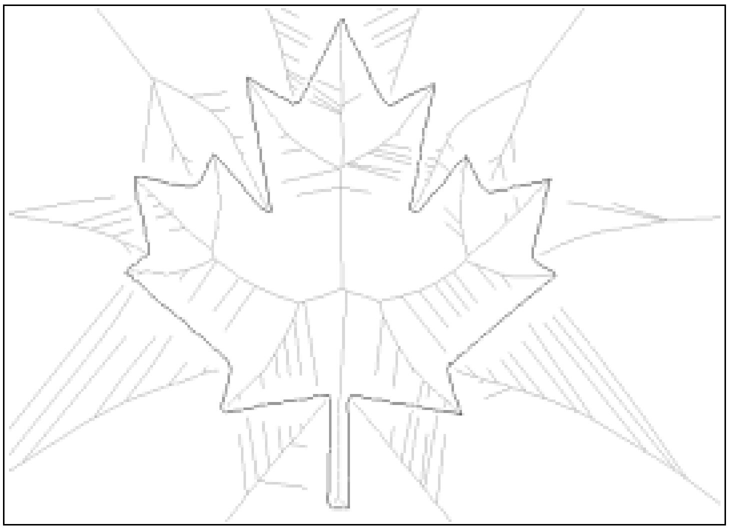

Figure 8 Crust and skeleton of the scanned boundary of a maple leaf

4. CURVE GENERALIZATION

The key idea applied here to generalization processes is the concept of *skeleton retraction*. The idea is quite simple - simpler objects have simpler skeletons, which means simpler shapes. (This is also true for the space between objects - retraction here simplifies the common Voronoi boundary between them.) This approach is only made possible because we can preserve the link between the skeleton and the crust. In fact, the process we have described so far is merely a labelling of the Delaunay and Voronoi edges, aided by the Quad-Edge/Quad-Arc data structure.

This paper only describes some of the initial steps in this controlled retraction process - that of retracting each leaf of the skeleton tree to the same location as its parent. This provides a skeleton with fewer branches, and a crust/boundary with fewer minor perturbations. Other retraction procedures are possible given certain knowledge rules about the desired shapes of the objects concerned. Some of these issues are discussed in Ogniewicz [15] and Ogniewicz and Ilg [16].

These spurious “hairs” on the generated skeletons are well-known artefacts of skeleton generation, where any irregularities in the boundary generate unwanted skeleton branches. Ogniewicz attempted to reduce skeletons formed from raster boundary points to a simple form by retracting the leaf nodes of the skeleton until a specified minimum circumcircle was achieved, but with the development of the one-step crust and skeleton algorithm, this process may be greatly simplified.

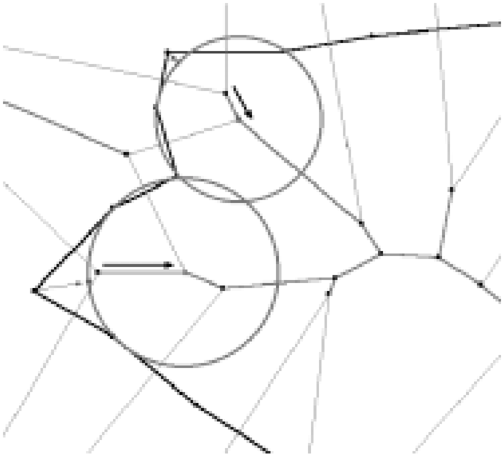

Figure 9 Skeleton retraction

Alt and Schwartzkopf [1], as well as Blum [4] showed that leaf nodes of a skeleton correspond to locations of minimum curvature on the boundary. For a sampled boundary curve this means that three adjacent points are cocircular, with their centre at the skeleton leaf. If we wish to simplify the skeleton we should retract leaf nodes to their parent node location. This means that we now have four cocircular points instead of three. The retraction is performed by taking the central point of the three defining the leaf node, and moving it towards the parent node of the skeleton until it meets the parent node circumcircle. This smoothes outward-pointing salients in the boundary of the object. The same should be done from the other side of the boundary, retracting those salients also. This may displace some of the points involved in the first smoothing step, but as the process is convergent a small number of iterations suffices to produce a smoothed curve having the same number of points as the original, but with a simplified skeleton, as shown in Figures 1 and 2. The retraction process is shown in Figure 9. Here, in order to retract the leaf node of the skeleton to its parent node, the exterior vertex is displaced radially onto the parent node circumcircle. Figure 10 shows the result of skeleton retraction for the maple leaf of Figure 7.

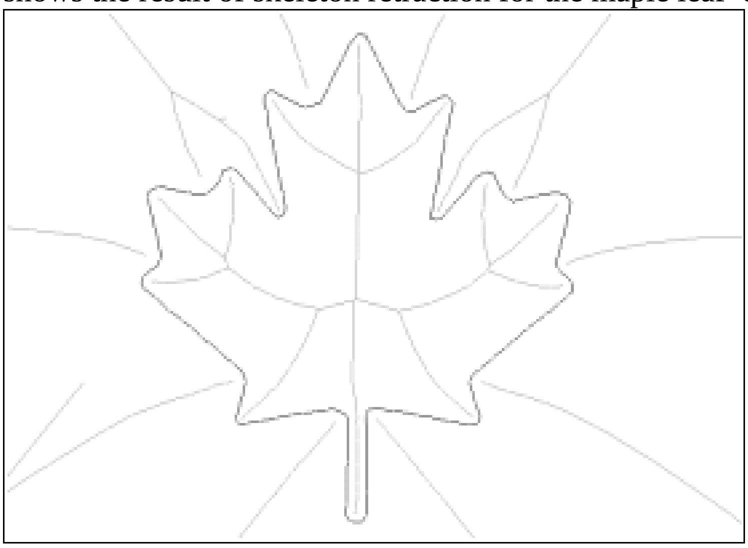

Figure 10 Smoothed crust and skeleton of Figure 7

This process is interesting for several reasons. Firstly, we have retracted the leaf nodes of the skeleton, greatly reducing its complexity. This then gives us a resulting skeleton closer to Blum's idea of the Medial Axis Transform, but without the artefacts due to perturbation of the samples along the "ideal" boundary. Blum's motivation was to provide stable descriptors of shape for "biological" objects, and the skeletons we have derived are well suited to that. However, retraction of skeleton leaves may be appropriate in the middle of a curve, but inappropriate at, for example, the corner of a building. Such boundary points would need to be flagged prior to the smoothing operation. Note that this smoothing process has no metric tolerance associated with it - so there is no problem with scale. Convergence is based on cocircularity. (This is particularly useful in the case of contour maps, as slope is perpendicular to the contour segments, so drainage is always towards skeleton nodes.)

Figure 11 Crust and skeleton of a simple contour map

Because of the symmetry between the endo- and exo-skeletons, there is no need to operate exclusively on closed curves – the process is equally effective considering both sides of an open curve. In addition, the skeleton may act as a linkage between adjacent objects - for example between adjacent curves of a contour map. The retraction process can not cause one curve to cross another (as can happen with simple curve smoothing), because the two crusts must have a separating skeleton. We thus get simplified curves that fit together. This is completely general, and provides a new model for map generalization. It is particularly relevant for contour map generalization or smoothing, because the usual one-dimensional curve smoothing procedures can not guarantee that adjacent contours do not overlap.

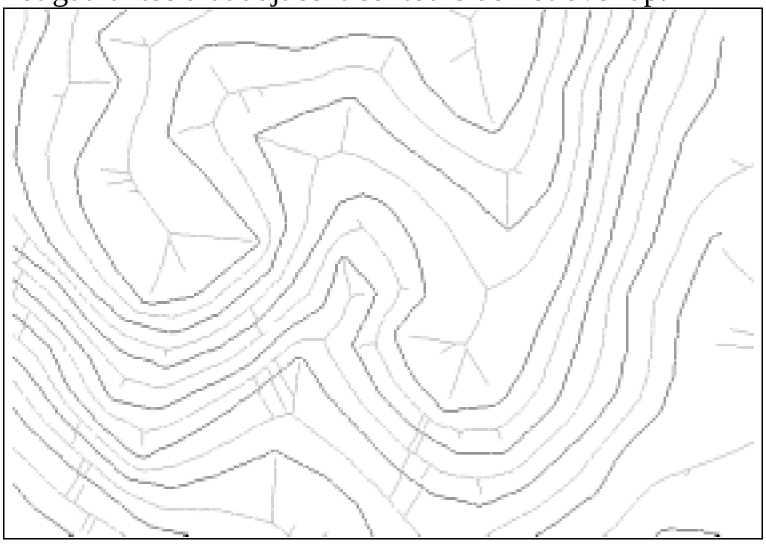

Figure 12 Smoothed version of Figure 11

Processing Contour Maps.

In the case of contour maps, the result consisted of a connected set of contours if the curves were sufficiently well sampled. In between each curve is a skeleton, or medial axis, consisting of the Voronoi edges separating curves or portions of curves. Figure 11 shows the crust and skeleton for a simple contour map, and Figure 12 shows the smoothed version of Figure 11. Figures 13 and 14 show enlargements of portions of those figures.

The remaining secondary branches of the skeleton in Figure 12 are valuable as they indicate the probable intermediate form of the surface between contours - such as minor ridges and valleys. Derived where there are re-entrants in a single contour, they approximate the human interpretation of the surface form, and can serve to improve runoff modelling. Note the cases where the skeleton “breaks through” the crust in Figure 11 due to the high local irregularities of the sampling of the curves. This has been reduced, but not eliminated, in Figure 12 as the skeleton retraction process is only guaranteed for an initially connected crust.

Figure 13 Detail of Figure 11

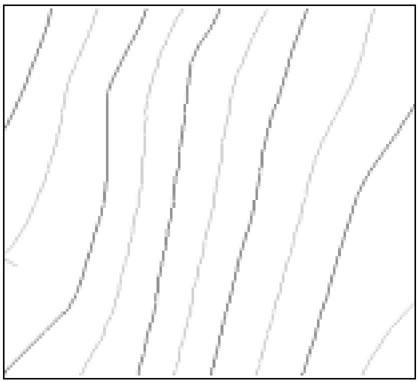

Figure 14 Detail of Figure 12

5. Contour Enrichment

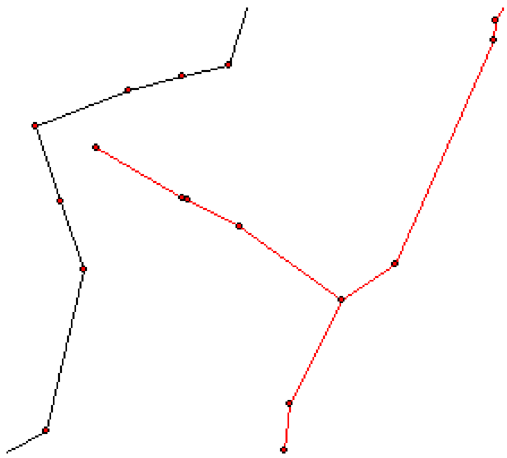

Figure 15 Skeleton branch

So far we have seen that we can generate a well-defined "crust" for each contour line, if it is well enough sampled, as well as the separating skeleton. Each of these is just a labelling of the appropriate Voronoi or Delaunay edges. Using the properties of the skeleton, we can smooth or generalize the contour lines without fear of overlapping arcs. However, the real advantages of the approach are seen when we look at the problem of "flat triangles".

Wherever three adjacent vertices along a contour have an empty circumcircle, a Voronoi vertex is generated. We retracted all such first-order vertices in the generalization process just described. However, Figures 12 and 15 show cases where the skeleton between a pair of contours is not just a simple curve. Here several points on the same contour form "flat triangles", and generate the Voronoi vertices of a branch of the main skeleton. From the insight of Amenta et al., the insertion of this skeleton branch into the triangulation is guaranteed to break up these triangles.

The resulting diagram of the crust and skeleton may then be processed to extract the terrain model. The enriched triangulation will consist of the triangulation of the original data points forming the crust, plus the Voronoi vertices that formed the skeleton. But first it is necessary to estimate the elevation at each skeleton vertex. In most cases this is straightforward: the skeleton is at the mid point between two contours, and hence its elevation is half way between. This can be detected because each skeleton point is a Voronoi vertex, which is the centre of a circumcircle touching three of the original contour data points. If these vertices do not have the same elevation, the skeleton is part of an intermediate contour, with an elevation half way between the originals. If they do have the same elevation we have the case of minor re-entrants or promontories, where there are branches of the skeleton separating the two parts of the contour curve, connecting the main skeleton to the head of the ridge or valley - or else we have a closed contour forming a peak or pit.

Various workers have worked on the problem of generating these intermediate points for an enriched triangulation. In particular, Aumann et al. [3] used raster techniques to estimate the skeleton of these re-entrants. In our case these are obtained automatically from the Voronoi/Delaunay construction, with the crust/skeleton classification. Figure 15 shows one detected valley. Each of these points is a Voronoi vertex, and its circumcircle touches both sides of the contour re-entrant. As minor valleys become narrower towards their heads, the radius of any skeleton point on the re-entrant, compared with the skeleton circle at the junction of the branch with the main medial skeleton, gives the elevation of skeleton point as a proportion of the elevations of the medial contour and the one forming the re-entrant. Figure 16 shows the method. If Zc is the elevation of the contour with the re-entrant, Zb is the elevation of the other contour, Zi the elevation of the skeleton point to be estimated, Rr the radius of the reference circle and Ri the radius of the skeleton point, then Zi = Zc – (Ri/Rr)*(Zc – Zb)/2. Figures 17 and 18 show two examples of values estimated in this way. As can be seen, the results are entirely plausible, and these enriching points may now be inserted into a new triangulation, along with the original data.

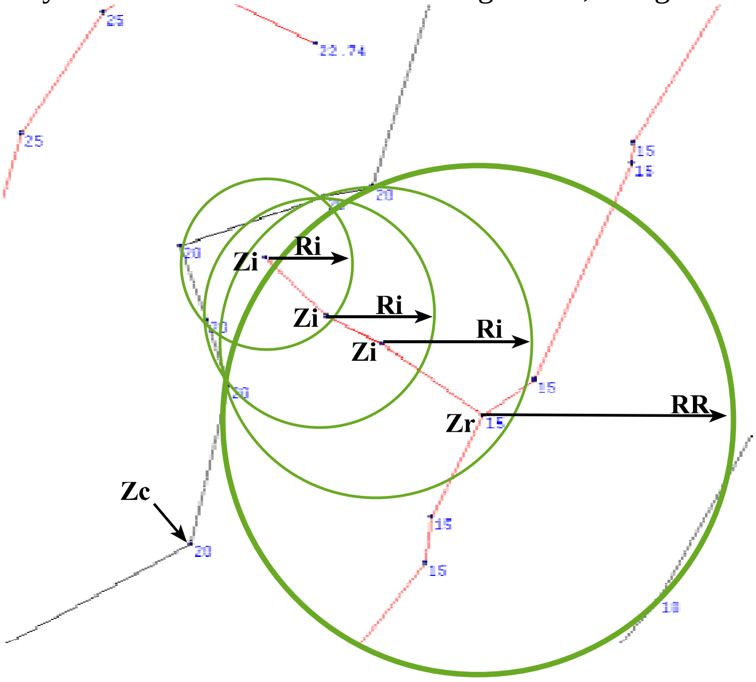

Figure 16 Skeleton point height estimation using circle ratios

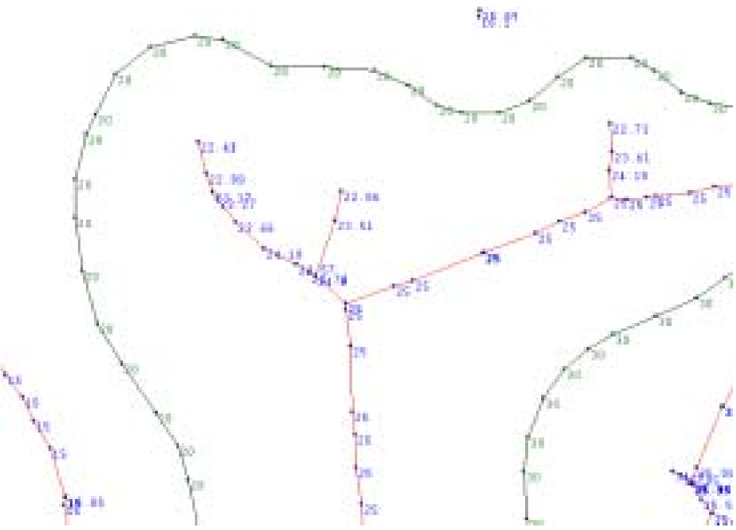

Figure 17 Skeleton height estimates

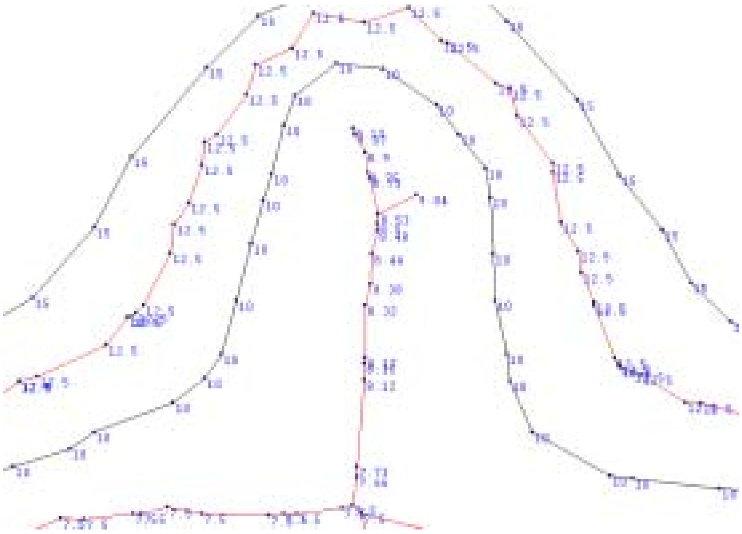

Figure 18 Skeleton height estimates

Figure 19 shows a perspective view of a terrain model constructed directly from the contour input. The “flat triangles” are clearly visible, and Figure 20 shows the resulting interpolated contours. Clearly the results are poor. However, when the skeleton points are added, as in Figure 21, the “flat triangles” have been removed, and the contours, shown in Figure 22, appear reasonable.

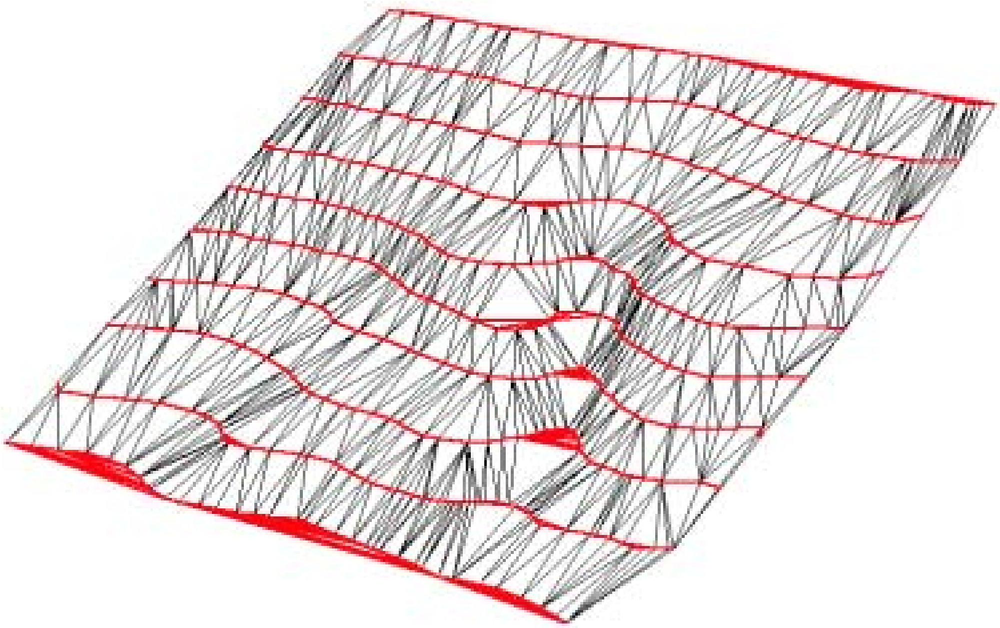

Figure 19 Perspective view of a simple triangulation of contour data

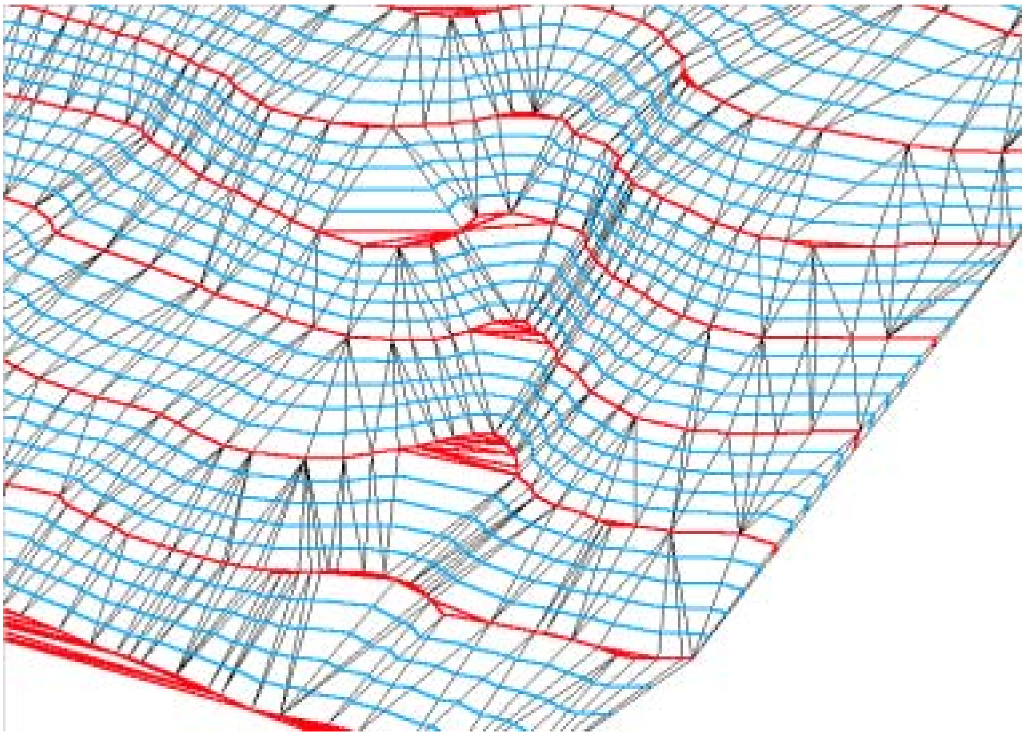

Figure 20 Contours interpolated from the triangulation of Figure 19

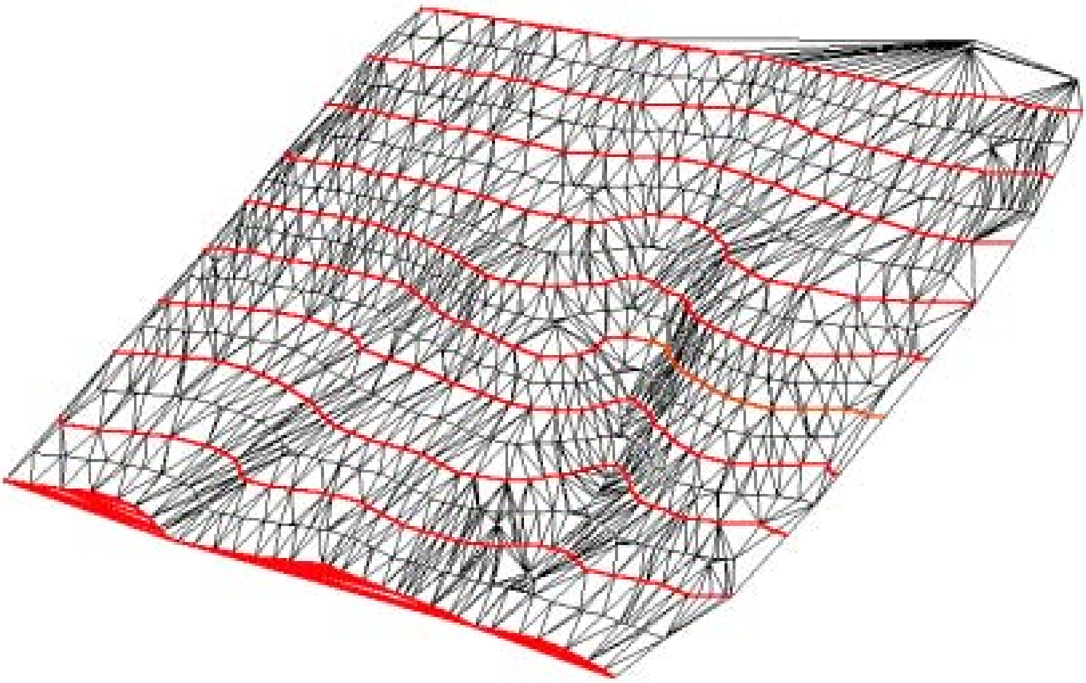

Figure 21 Triangulation of the enriched data of Figure 19

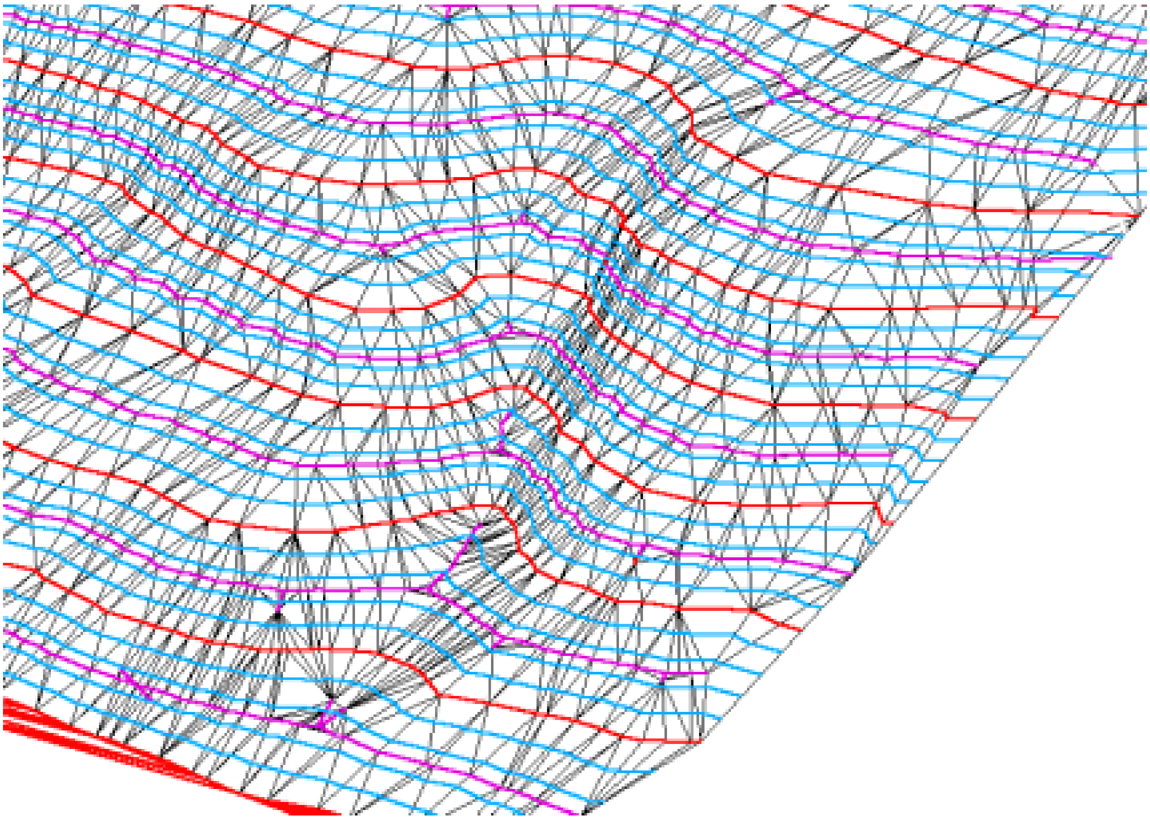

Figure 22 Contours interpolated from the triangulation of Figure 21

Peaks and Pits

Nevertheless, not all cases of “flat triangles” can be solved in this fashion. Figure 23 shows the triangulation of a summit – there are flat triangles here too. We may, however, use the same approach if we remember that every crust segment is a Delaunay edge with its dual Voronoi edge suppressed. Because it is a crust segment it has an empty circle, with Voronoi vertices on each side of it (see Figure 5). Each of these Voronoi vertices has the usual circumcircle and, as before, if we assume linear relationships, the ratio of the radii gives the ratio of the elevation differences. (It should be remembered that this calculation is being performed along the line of maximum slope, perpendicular to the contour segment that forms the crust. Hence we also have a good initial slope model for runoff calculations or similar exercises.)

In Figure 24 the northeast branch of the skeleton of the summit is a Voronoi vertex connected to another Voronoi vertex on the 35 m skeleton. The ratio of the radii of the circumcircles of these two Voronoi vertices gives the ratio of the elevations – and hence the elevation of that summit skeleton vertex. Given this one value, the usual ratio of the radii may be used to estimate the remaining summit skeleton values. This approach is surprisingly insensitive to the choice of the initial leaf vertex of the summit (or pit) skeleton. Figure 25 shows the result of a test data set where the southeast leaf was used, and in Figure 26 the (minor) southern leaf was the reference vertex.

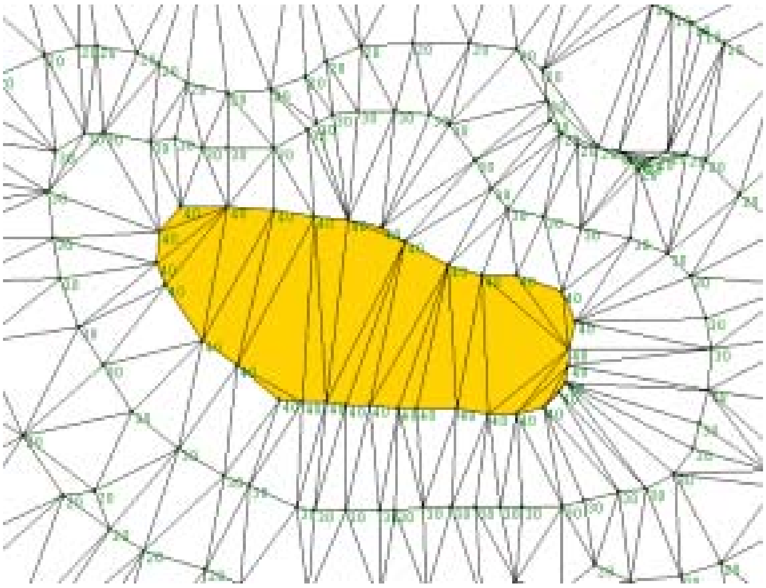

Figure 23 Triangulation of a summit region

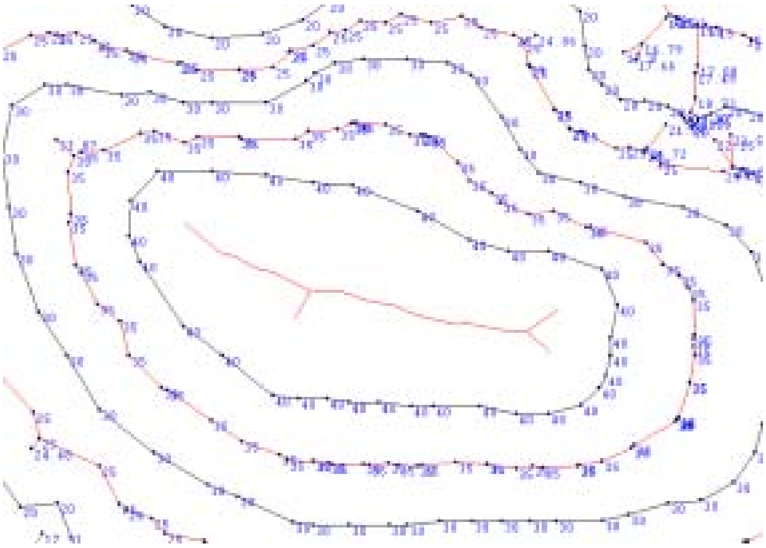

Figure 24 Skeleton of Figure 23

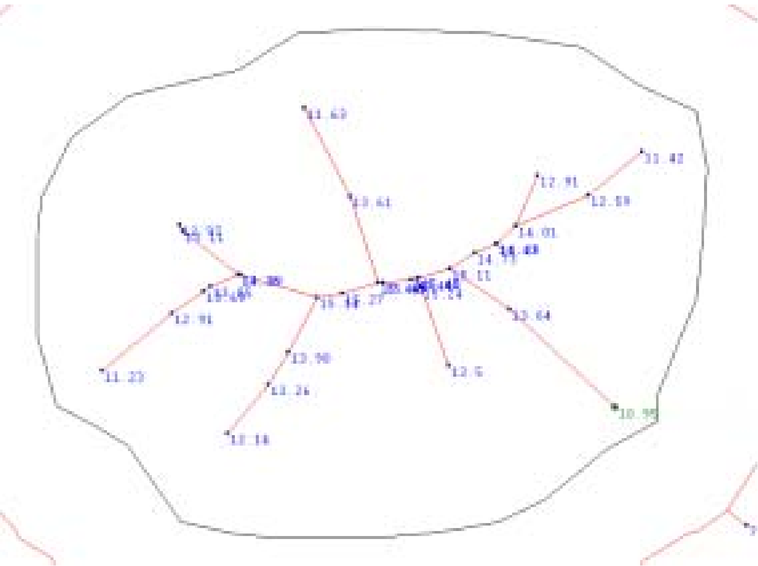

Figure 25 Estimated summit skeleton values using the southeast leaf as the reference vertex

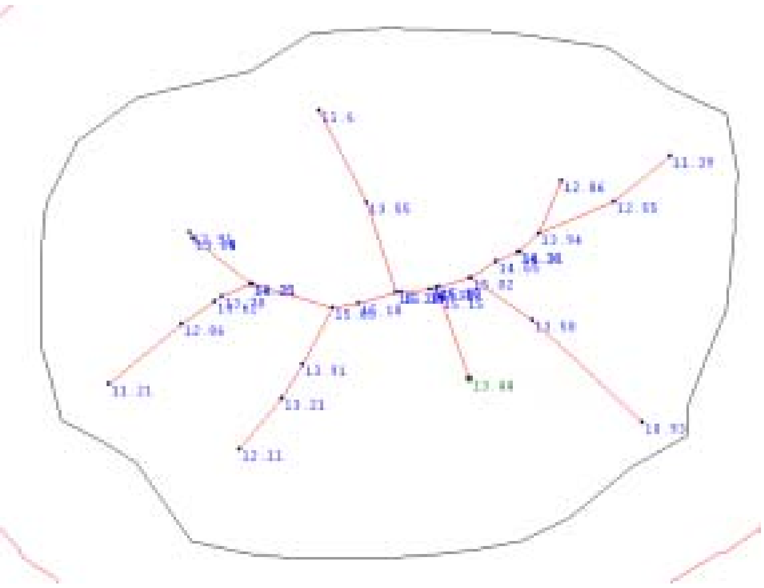

Figure 26 Estimated summit skeleton values using the minor southern leaf as the reference vertex

Comparisons with other methods

While the real-world examples used in this article appear convincing, we wanted to test this against well-known commercial methods – in this case the usual inverse-distance weighting interpolation, and a fairly simple kriging option. In both cases the commercial software produced a grid that could be viewed. Figure 27 shows an extreme case of a valley expressed by a heavily re-entrant contour line. The flat triangles are clearly visible. Figure 28 shows the results for the inverse distance method, and Figure 29 shows the results of the kriging approach – which are somewhat better, but which are still incapable of handling the apparent flat regions. Figure 30 shows the result of adding the skeleton vertices to the triangulation, as described here, and using "area-stealing" interpolation [7] based on the Voronoi cells, to fill in within the initial triangles. While not an exact comparison, the results show that the proposed methods achieve the desired results, where the other available methods did not.

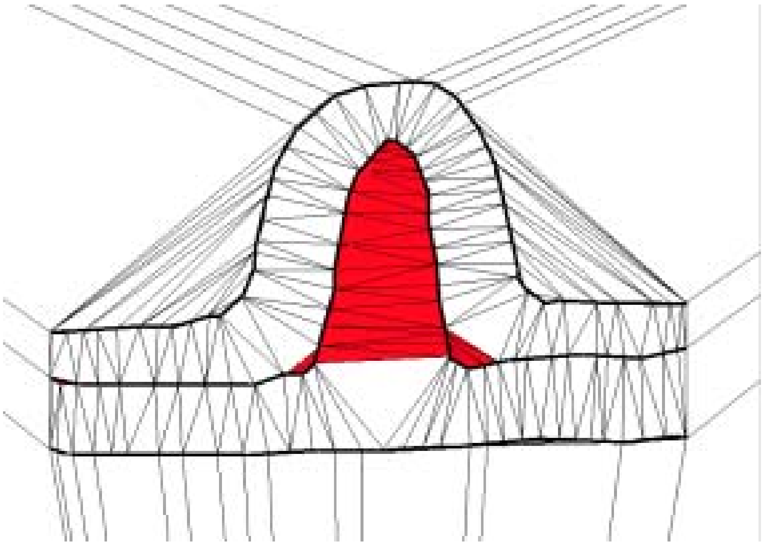

Figure 27 A synthetic "extreme" re-entrant contour

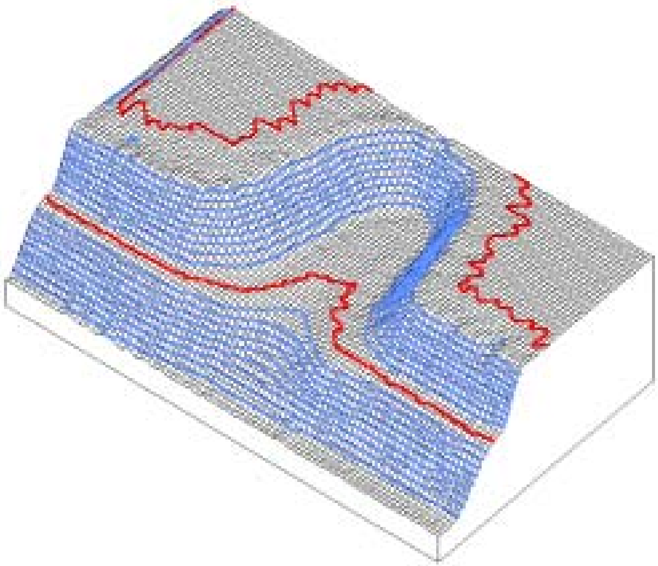

Figure 28 Inverse-distance grid interpolation for the data of Figure 27

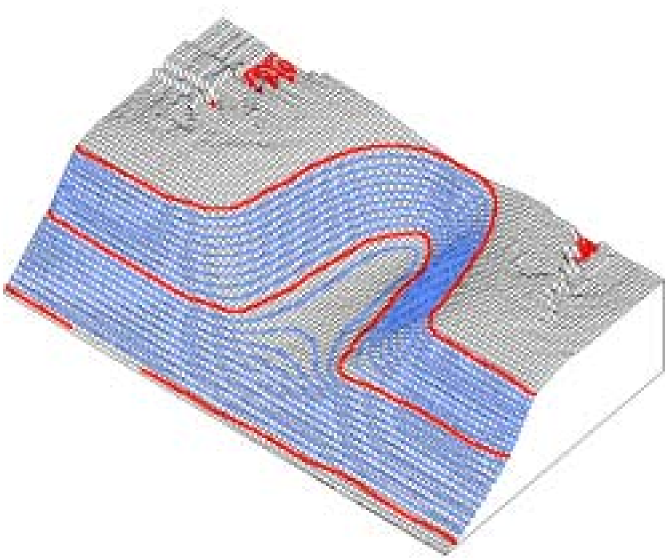

Figure 29 Simple kriging grid interpolation for the data of Figure 27

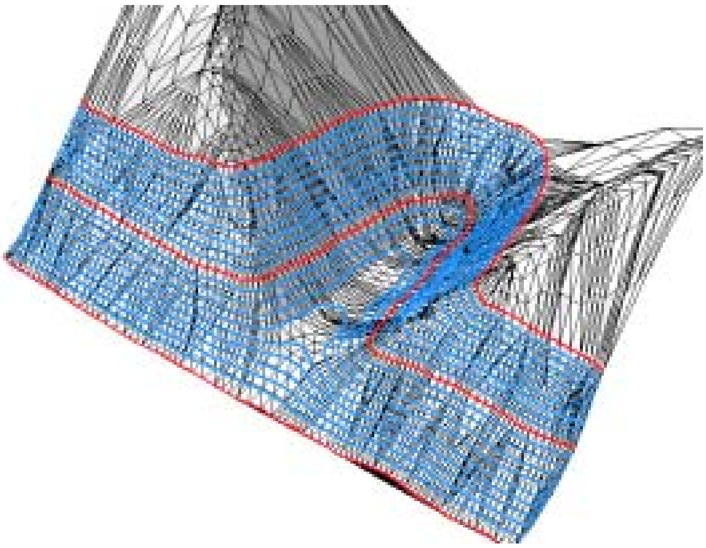

Figure 30 Area-stealing interpolation for the enriched data of Figure 27

Conclusions and Future Work

On the basis of the crust/skeleton model just described, it is possible to build the components of a reasonable TIN model, using information about the supplementary skeleton points and the slope at contour segments. This is consistent with human interpretation of the original contours. Slope values at contour segments are also valuable for the generation of slope maps or other derived products. If a grid is desired, the area-stealing interpolation method may be used on the original data, the slopes at data points, plus the intermediate Voronoi vertices if required. If a triangulation is the preferred model, then the Voronoi vertices may be used to densify the original triangulation of the contour data. In each case the crust/skeleton model takes advantage of the human judgement implicit in the original contour construction, and mimics human interpretation of ridges, valleys and slopes, while preserving the basic topological consistency of the original data.

7. REFERENCES

[1] Alt, H. and O. Schwarzkopf. “The Voronoi diagram of curved objects”, Proceedings, 11th Annual ACM Symposium on Computational Geometry, 89-97, 1995.

[2] Amenta, N., M. Bern and D. Eppstein. “The crust and the beta-skeleton: combinatorial curve reconstruction”, Graphical Models and Image Processing, Vol. 60:125-135, 1998.

[3] Aumann, G., H. Ebner, and L. Tang. “Automatic derivation of skeleton lines from digitized contours”, ISPRS Journal of Photogrammetry and Remote Sensing, Vol. 46:259-268, Elsevier Science Publishers B.V., Amsterdam, 1991.

[4] Blum, H. “A transformation for extracting new descriptors of shape”, In: W. Whaten Dunn (ed.), Models for the Perception of Speech and Visual Form, MIT Press, Cambridge, Mass., 153-171, 1967.

[5] Carrara, A., G. Bitelli, and R. Carla. “Comparison of techniques for generating digital terrain models from contour lines”, International Journal of Geographical Information Science, Vol.11: 451-473, 1997.

[6] Garcia, A.B., C.G. Nicieza, J.B.O. Mereé, and A.M. Diaz. “A contour line based triangulating algorithm”, Proceedings, 5th International Symposium on Spatial Data Handling, 273-284, 1990.

[7] Gold, C.M. “Chapter 3 - Surface interpolation, spatial adjacency and G.I.S”, in: Three Dimensional Applications in Geographic Information Systems (J. Raper, ed.), Taylor and Francis, Ltd., London, 21-35, 1989.

[8] Gold, C.M. “Simple topology generation from scanned maps”, Proceedings, Auto-Carto 13, ACM/ASPRS, Seattle, April, 337-346, 1997.

[9] Gold, C.M. “The Quad-Arc data structure” in: Poiker, T.K. and Chrisman,N.R. (eds.). Proceedings, 8th International Symposium on Spatial Data Handling, Vancouver, BC, 713-724, 1998.

[10] Gold, C.M. “Crust and anticrust: a one-step boundary and skeleton extraction algorithm”, in Proceedings of the ACM Conference on Computational Geometry, Miami, Florida, 189-196, 1999.

[11] Gold, C.M. and Snoeyink, J. “A one-step crust and skeleton extraction algorithm”, Algorithmica, (in press).

[12] Gold, C.M., J. Nantel and W. Yang. “Outside-in: an alternative approach to forest map digitizing”, International Journal of Geographical Information Systems, Vol. 10:291-310, 1996.

[13] Gold, C.M., D. Thibault and Z. Liu. Map Generalization by Skeleton Retraction. ICA Workshop on Map Generalization, Ottawa, August 1999.

[14] Guibas, L. and J. Stolfi. “Primitives for the manipulation of general subdivisions and the computation of Voronoi diagrams”, Transactions on Graphics, Vol. 4:74-123, 1985.

[15] Ogniewicz, R.L. “Skeleton-space: a multiscale shape description combining region and boundary information”, Proceedings on Computer Vision and Pattern Recognition, 746-751, 1994.

[16] Ogniewicz, R. and M. Ilg. “Skeletons with Euclidian metric and correct topology and their application in object recognition and document analysis”, Proceedings of the 4th International Symposium on Spatial Data Handling, Vol. 1:15-24, 1990.

[17] Okabe, A., B. Boots and K. Sugihara. Spatial Tessellations - Concepts and Applications of Voronoi Diagrams. John Wiley and Sons, Chichester. 1992

[18] Robinson, G.J. “The accuracy of digital elevation models derived from digitised contour data”, Photogrammetric Record, Vol. 14:805-814, 1994.

[19] Weibel, R., M. Heller. “Digital terrain Modelling”, in: Maguire, D.J., M.F. Goodchild, and D.W. Rhind, (eds.) Geographical Information Systems: Principles and applications, London; Longman, 1990.